Supporting Information to

Modulating between 2e$^-$ and 4e$^-$ pathway in the oxygen reduction reaction with laser-synthesized iron oxide-grafted nitrogen-doped carbon

Huize Wang, Maria Jerigova, Jing Hou, Nadezda V. Tarakina, Simon Delacroix, Nieves Lopez-Salas, Volker Strauss

Chemical composition S2
Electrical properties S3
Pre-Carbonization S3
X-ray photoelectron spectroscopy S5
STEM and EDX analysis S11
Oxygen reduction reaction performance S12
Comparison with published studies S14
References S15

Chemical composition

Table S1. *Elemental mass percentage of* ***pre-NC(Fe)_1(x)*** *and* ***LP-NC(Fe)_n(x)*** *obtained from combustion elemental analysis (N,C,H) and ICP-MS (Fe).**

sample	N	C	H	Fe
CNFA (CA/U300)	13	68	1	-
pre-NC(Fe)_1(2.3)	21	48	3	2.3
pre-NC(Fe)_1(2.7)	19	42	3	2.7
pre-NC(Fe)_1(8.6)	21	42	3	8.6
LP-NC(Fe)_1(3.0)	10	72	1	3.0
LP-NC(Fe)_1(4.6)	7	72	1	4.6
LP-NC(Fe)_1(12.1)	6	60	1	12.1
LP-NC(Fe)_2(3.3)	13	60	2	3.3
LP-NC(Fe)_2(3.8)	11	67	2	3.8
LP-NC(Fe)_2(14.5)	8	60	1	14.5

** The remaining mass is due oxygen.*

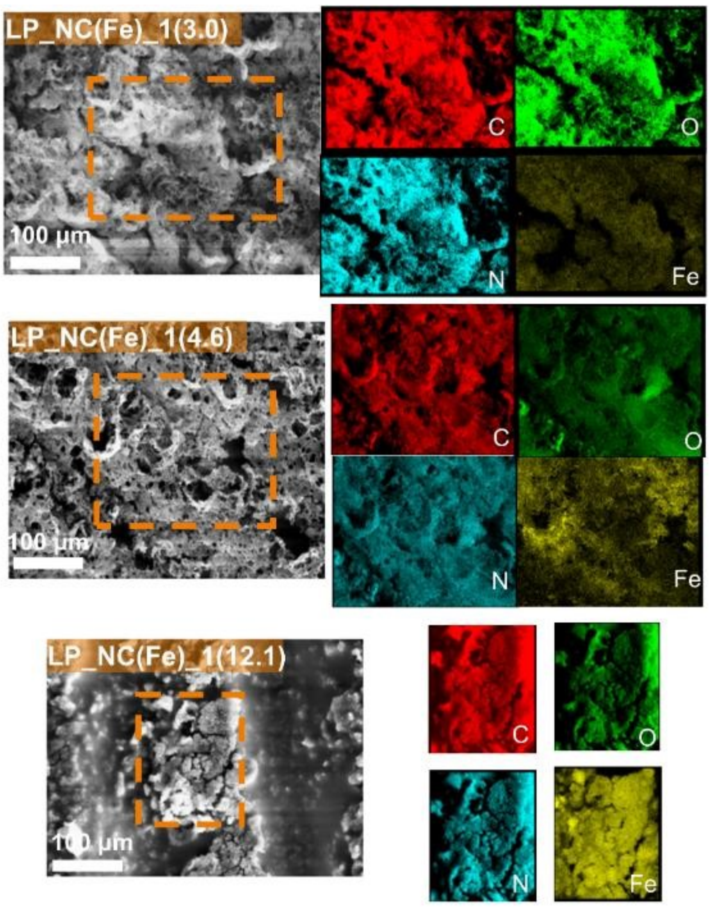

Figure S1. *EDX mapping of* ***LP_NC(Fe)_1(3.0)****,* ***LP_NC(Fe)_1(4.6)*** *and* ***LP_NC(Fe)_1(12.1)****.*

Electrical properties

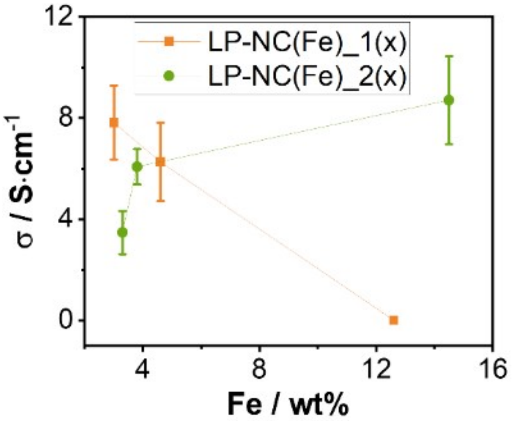

***Figure S2**. Electrical conductivity of films **LP-NC(Fe)_1(x)** and **LP-NC(Fe)_2(x)** obtained by averaging 30 sample films.*

Pre-Carbonization

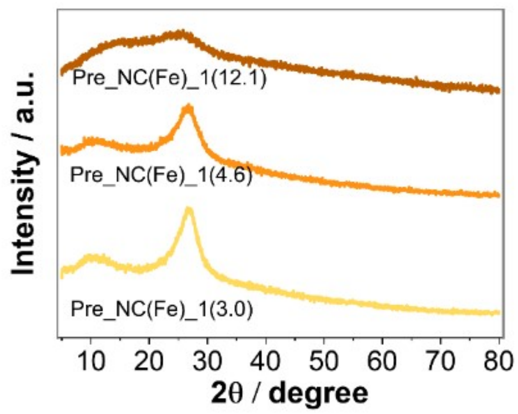

***Figure S3.** X-ray powder diffraction patterns of the primary films to route 1 (**pre-NC(Fe)_1(y)**), pre-carbonized at 300 °C.*

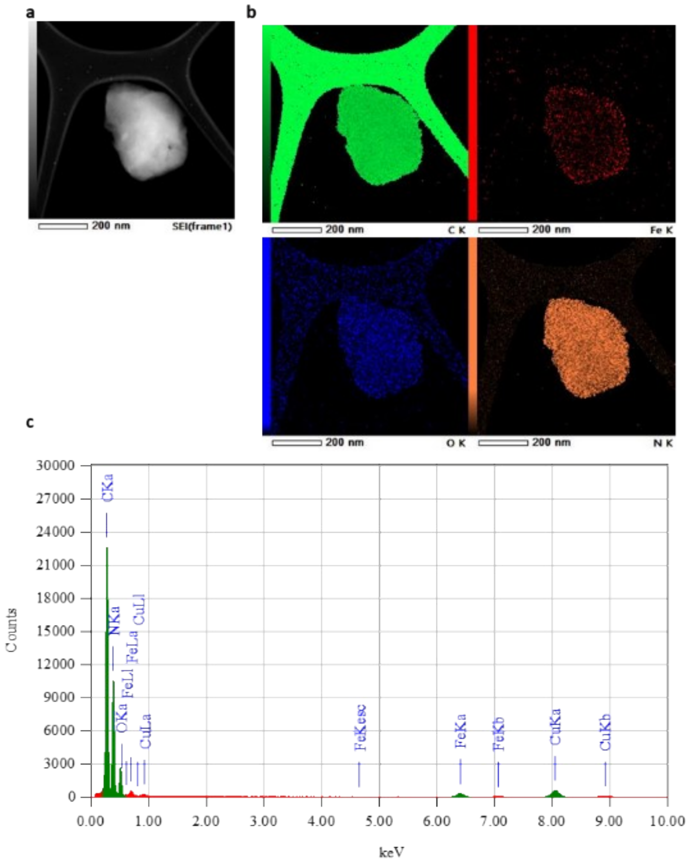

Figure S4. *(a) STEM-ADF images of* ***pre_NC(Fe)_1(3.0)****; (b)corresponding EDX elemental mappings and spectrum from (a).*

X-ray photoelectron spectroscopy

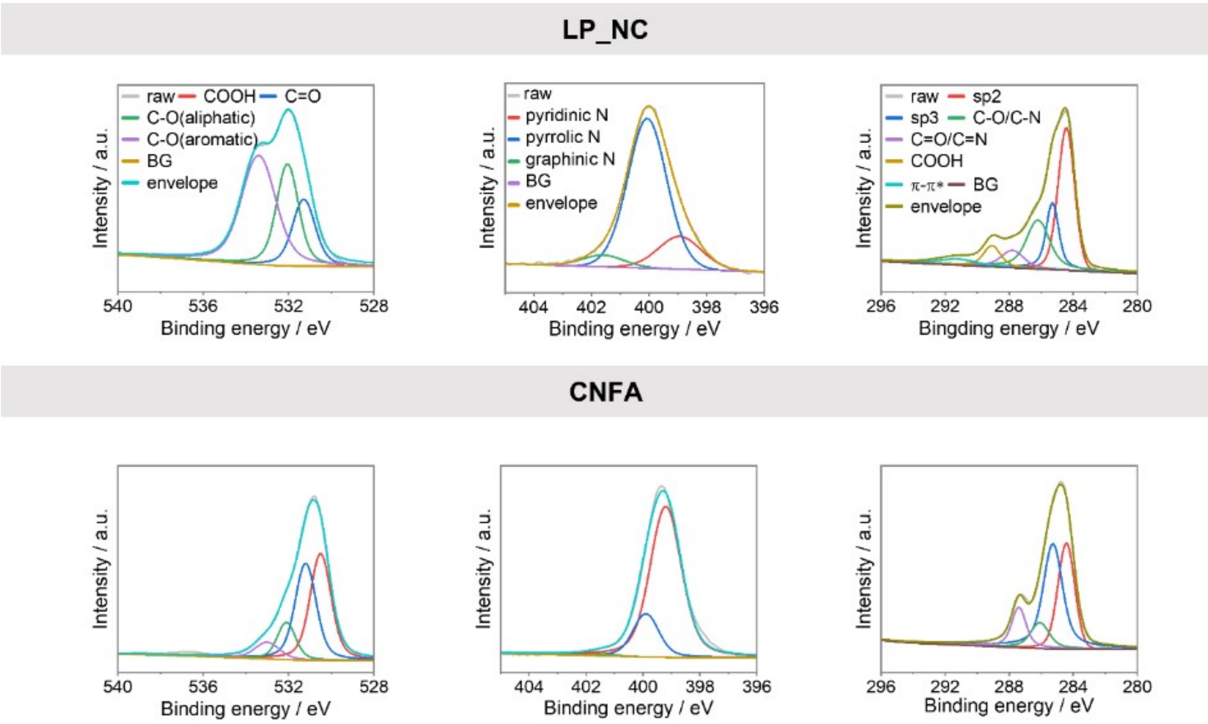

Figure S5. *XPS spectra of* ***LP_NC*** *(reference) and the* ***CNFA*** *(CA/U(300)) with emphasis on the* O_{1s} *(left),* N_{1s} *(middle), and* C_{1s} *regions (right).*

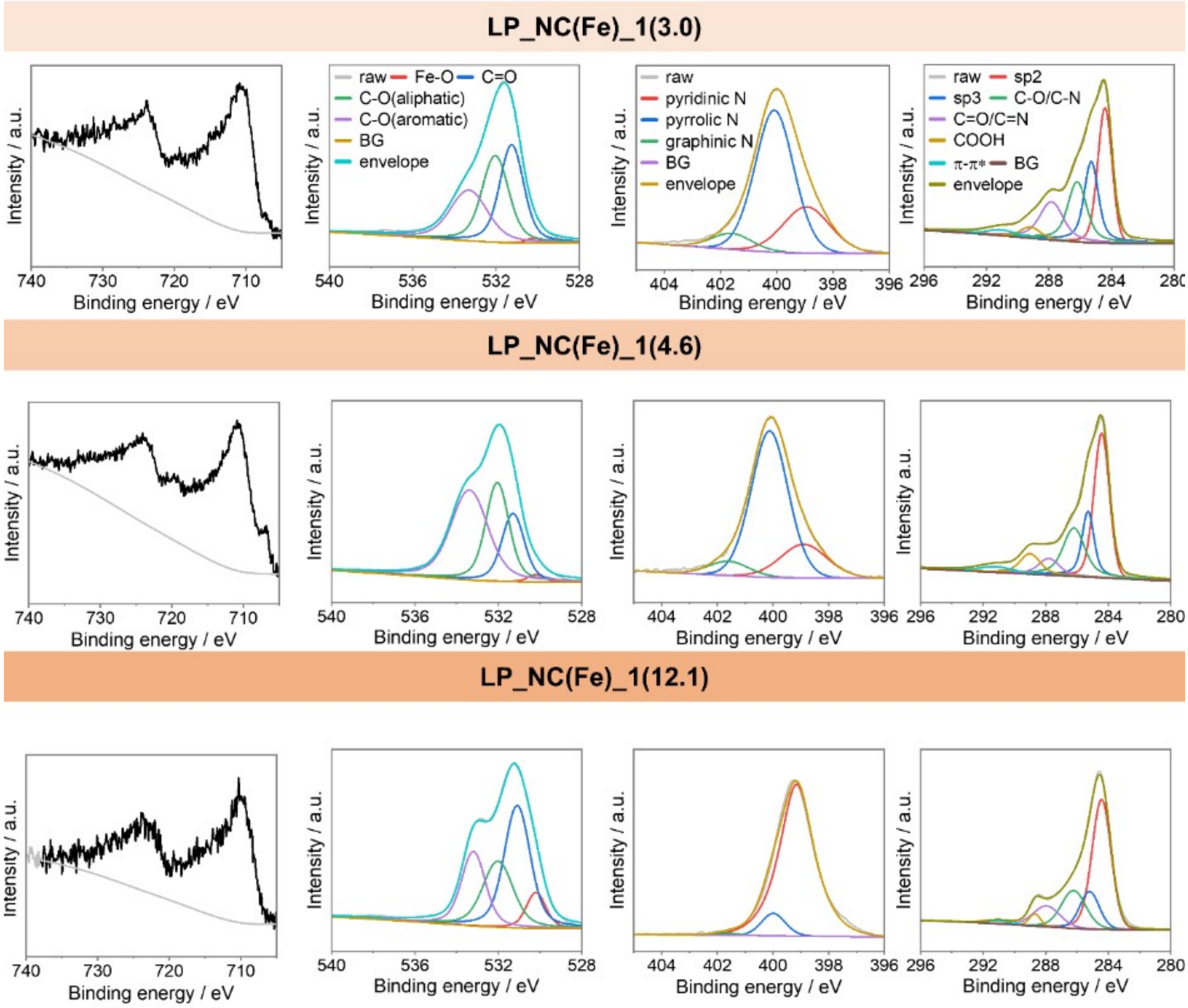

Figure S6. *XPS spectra of the samples prepared by route 1:* ***LP_NC(Fe)_1(3.0)****,* ***LP_NC(Fe)_1(4.6)*** *and* ***LP_NC(Fe)_1(12.1)*** *with emphasis on the F_{2p}, O_{1s}, N_{1s}, and C_{1s} (from left to right) regions.*

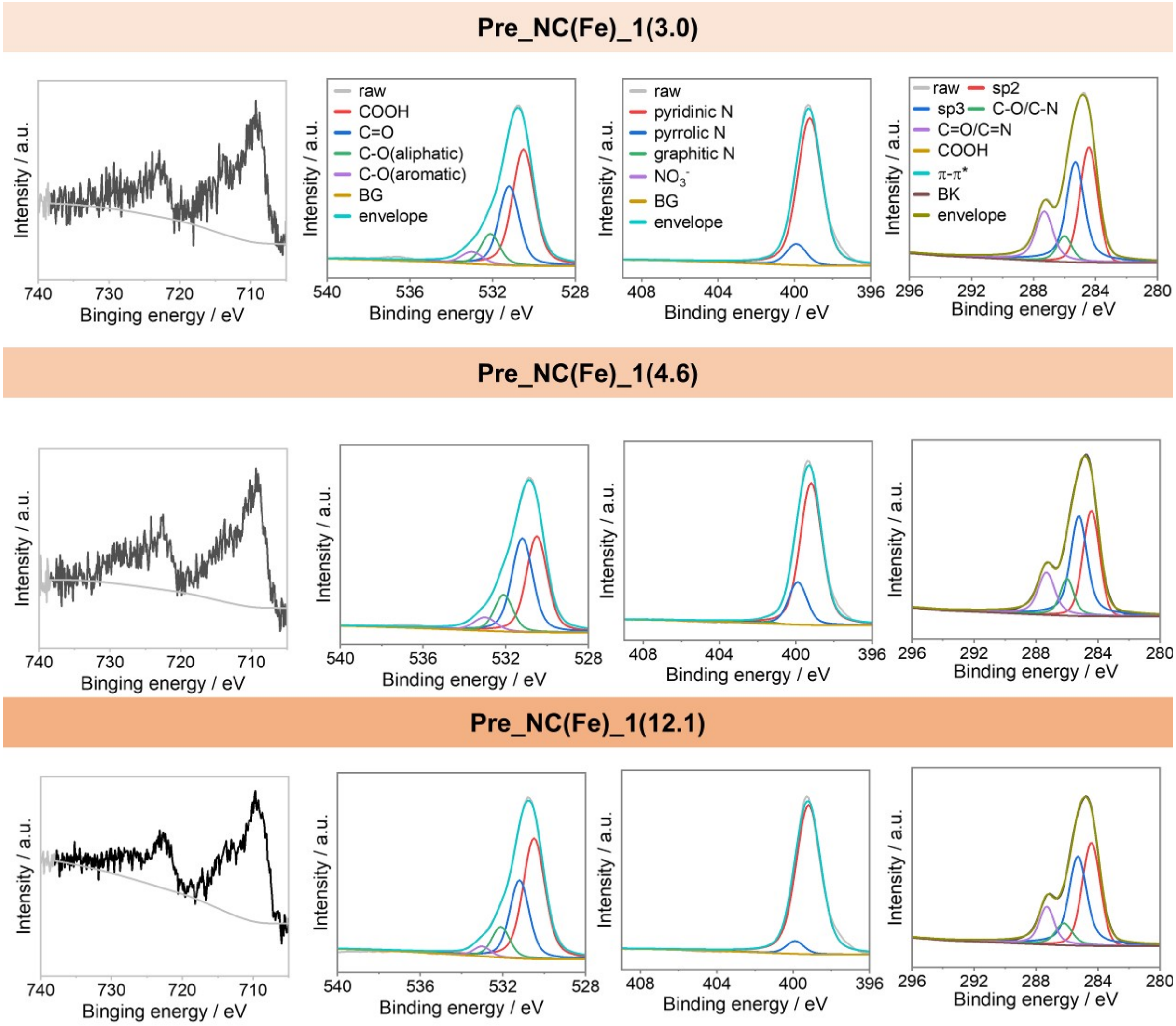

Figure S7. *XPS spectra of the primary films of route 1:* ***pre_NC(Fe)_1(3.0)****,* ***pre_NC(Fe)_1(4.6)*** *and* ***pre_NC(Fe)_1(12.1)*** *with emphasis on the* F_{2p}*,* O_{1s}*,* N_{1s}*, and* C_{1s} *(from left to right) regions.*

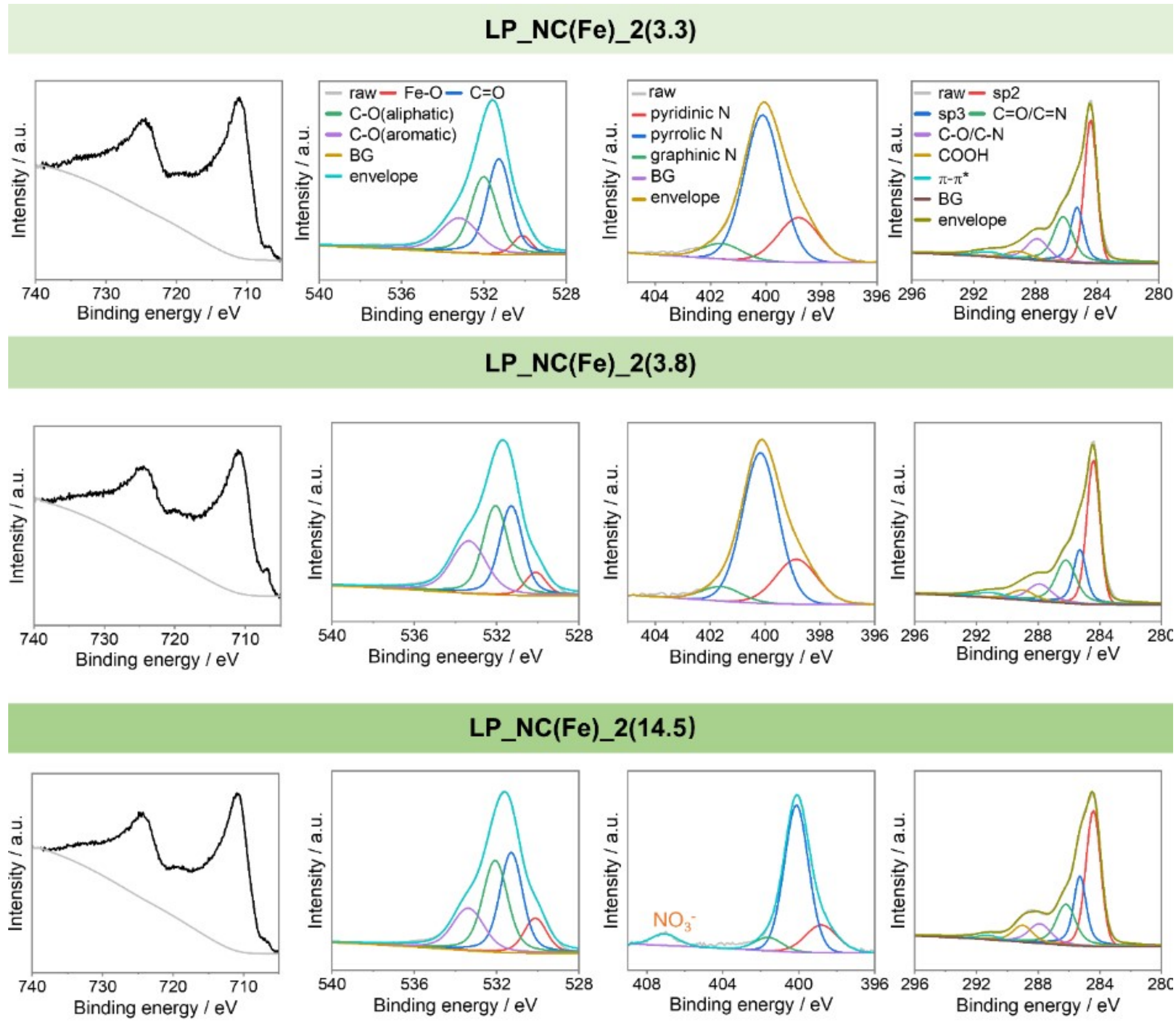

Figure S8. *XPS spectra of the samples prepared by route 2:* ***LP_NC(Fe)_2(3.3)****,* ***LP_NC(Fe)_2(3.8)*** *and* ***LP_NC(Fe)_2(14.5)*** *with emphasis on the F_{2p}, O_{1s}, N_{1s}, and C_{1s} (from left to right) regions.*

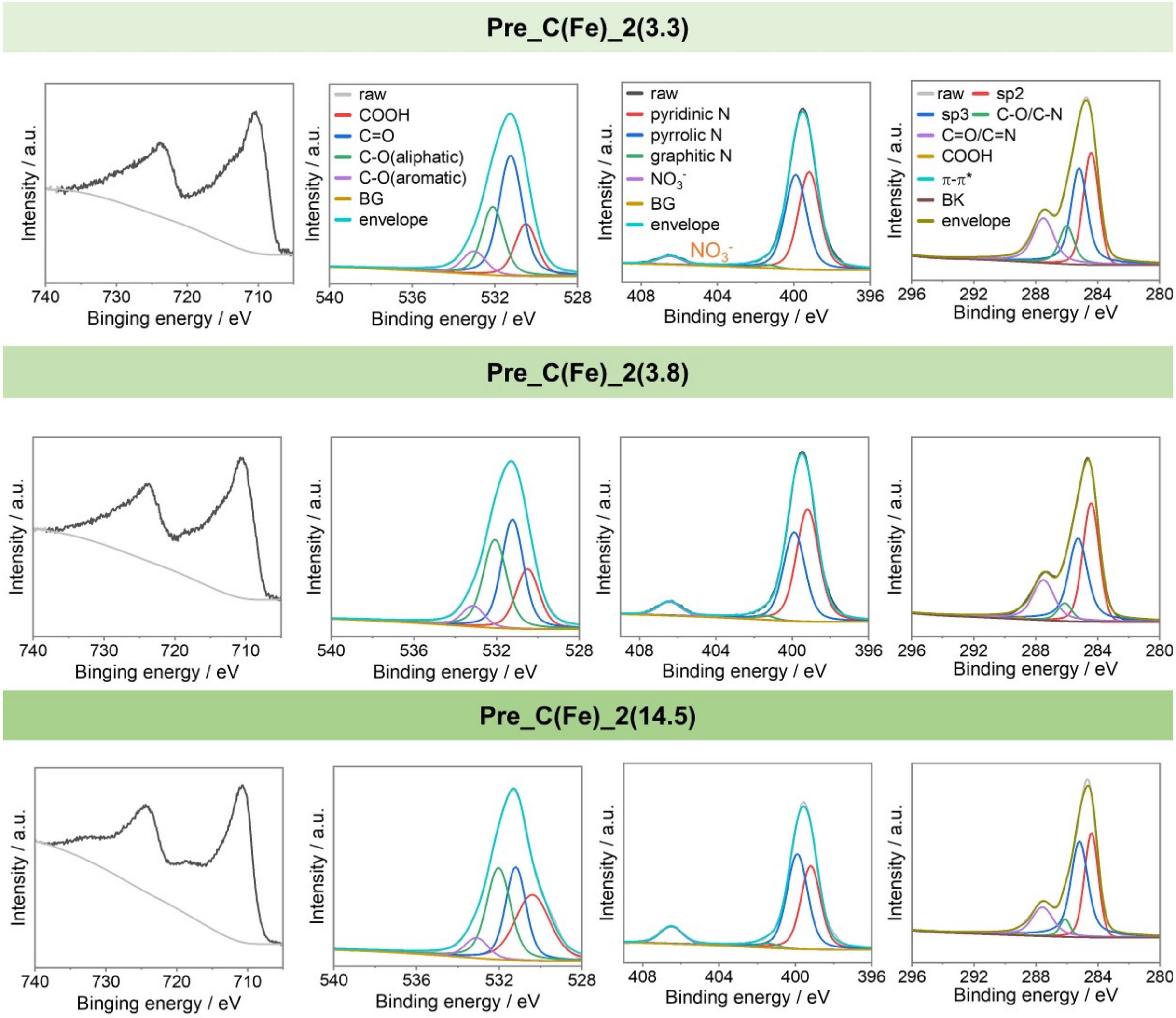

Figure S9. *XPS spectra of the primary films of route 2:* ***pre_NC(Fe)_2(3.3)****,* ***pre_NC(Fe)_2(3.8)*** *and* ***pre_NC(Fe)_2(14.5)*** *with emphasis on the F_{2p}, O_{1s}, N_{1s}, and C_{1s} (from left to right) regions.*

Table S2. *Elemental mass percentage of pre-NC(Fe)_1(x) and LP-NC(Fe)_n(x) obtained from XPS survey spectra quantification*

Sample	N	C	O	Fe
LP-NC	5.05	77.54	17.41	-
pre-NC(Fe)_1(2.3)	13.63	69.21	17.08	0.09
pre-NC(Fe)_1(2.7)	12.06	71.03	16.78	0.13
pre-NC(Fe)_1(8.6)	12.92	70.63	16.10	0.35
LP-NC(Fe)_1(3.0)	9.77	77.24	12.82	0.74
LP-NC(Fe)_1(4.6)	4.11	75.42	15.53	0.96
LP-NC(Fe)_1(12.1)	6.33	74.58	18.96	0.56
LP-NC(Fe)_2(3.3)	7.05	72.43	14.74	5.78
LP-NC(Fe)_2(3.8)	5.25	73.02	16.48	5.25
LP-NC(Fe)_2(14.5)	3.02	61.29	23.92	11.77

Table S3. *Composition of nitrogen of laser-carbon obtained by deconvolution of the N_{1s} peaks of the XPS spectra*

Sample	N_{1s} peaks (% of total peak area)				H_2O_2 production
	Pyridinic N	Pyrrolic N	Graphitic N	NO_3^-	
LP-NC	18.36	75.34	6.29	-	60
LP-NC(Fe)_1(3.0)	26.21	65.98	7.80	-	40
LP-NC(Fe)_1(4.6)	20.71	71.61	7.68	-	
LP-NC(Fe)_1(12.1)	90.83	8.44	0.73	-	2
LP-NC(Fe)_2(3.3)	25.37	67.50	6.93	-	80
LP-NC(Fe)_2(3.8)	21.22	68.09	10.70	-	
LP-NC(Fe)_2(14.5)	42.01	50.49	2.12	5.37	8

STEM and EDX analysis

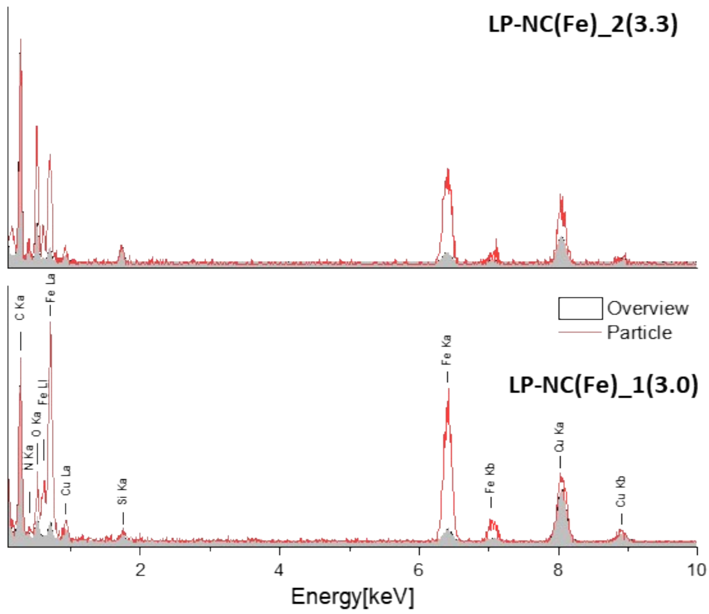

Figure S10. *EDX spectrum on overview (grey filling) and particle (red line) regions of* ***LP_NC(Fe)_1(3.0)*** *(bottom) and* ***LP_NC(Fe)_2(3.3)*** *(top).*

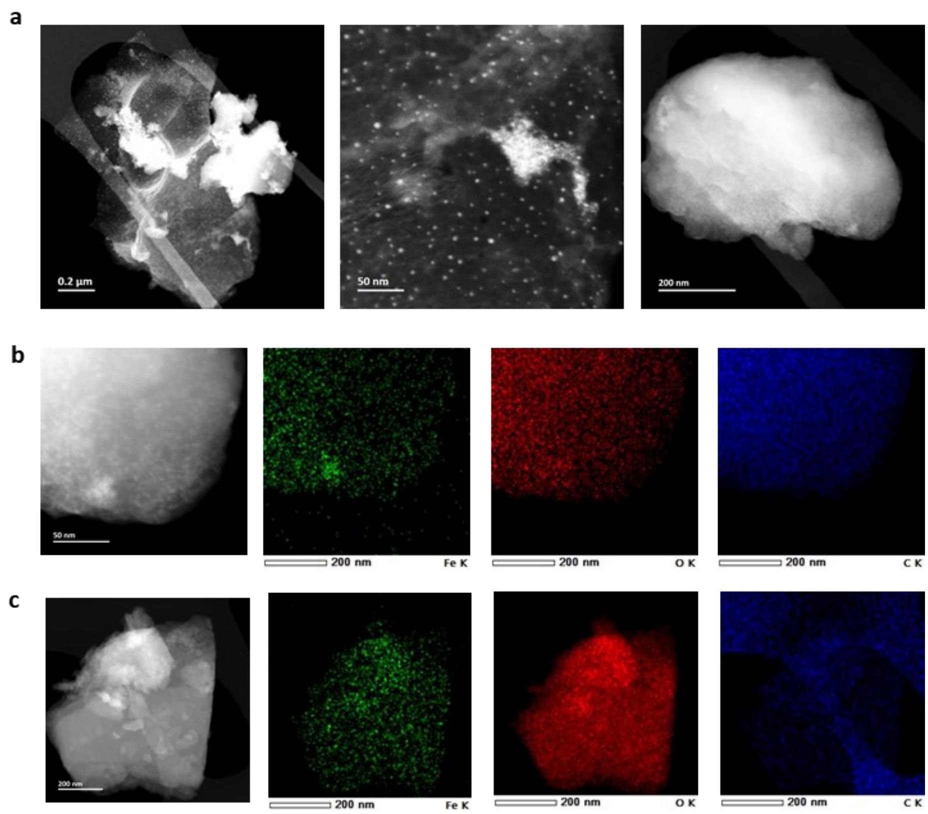

Figure S11. *(a) STEM image of thin film, clusters, and dense substrate (from left to right)from* ***LP_NC(Fe)_2(3.3)****; (b) EDX of dense carbon substrate grafted with iron clusters; (c) EDX with solid flake containing iron and oxide.*

Oxygen reduction reaction performance

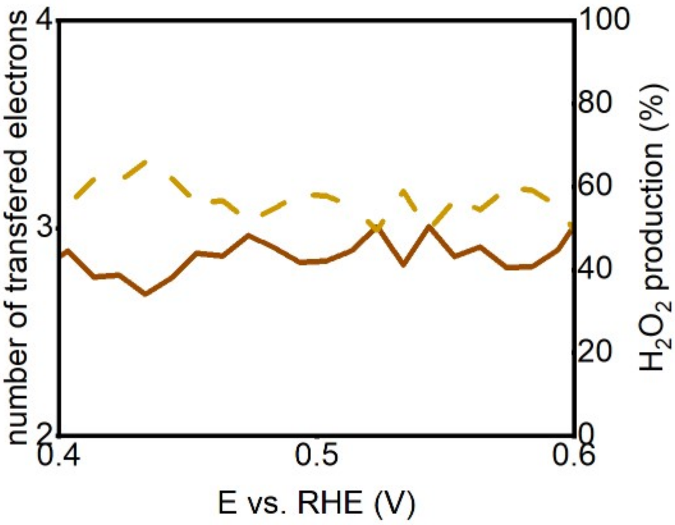

Figure S12. *Calculated number of transferred electrons and H_2O_2 production efficiency of LP-C(Fe)_2(3.8) in KOH 0.1M. H_2O_2 production (%) in dashed lines.*

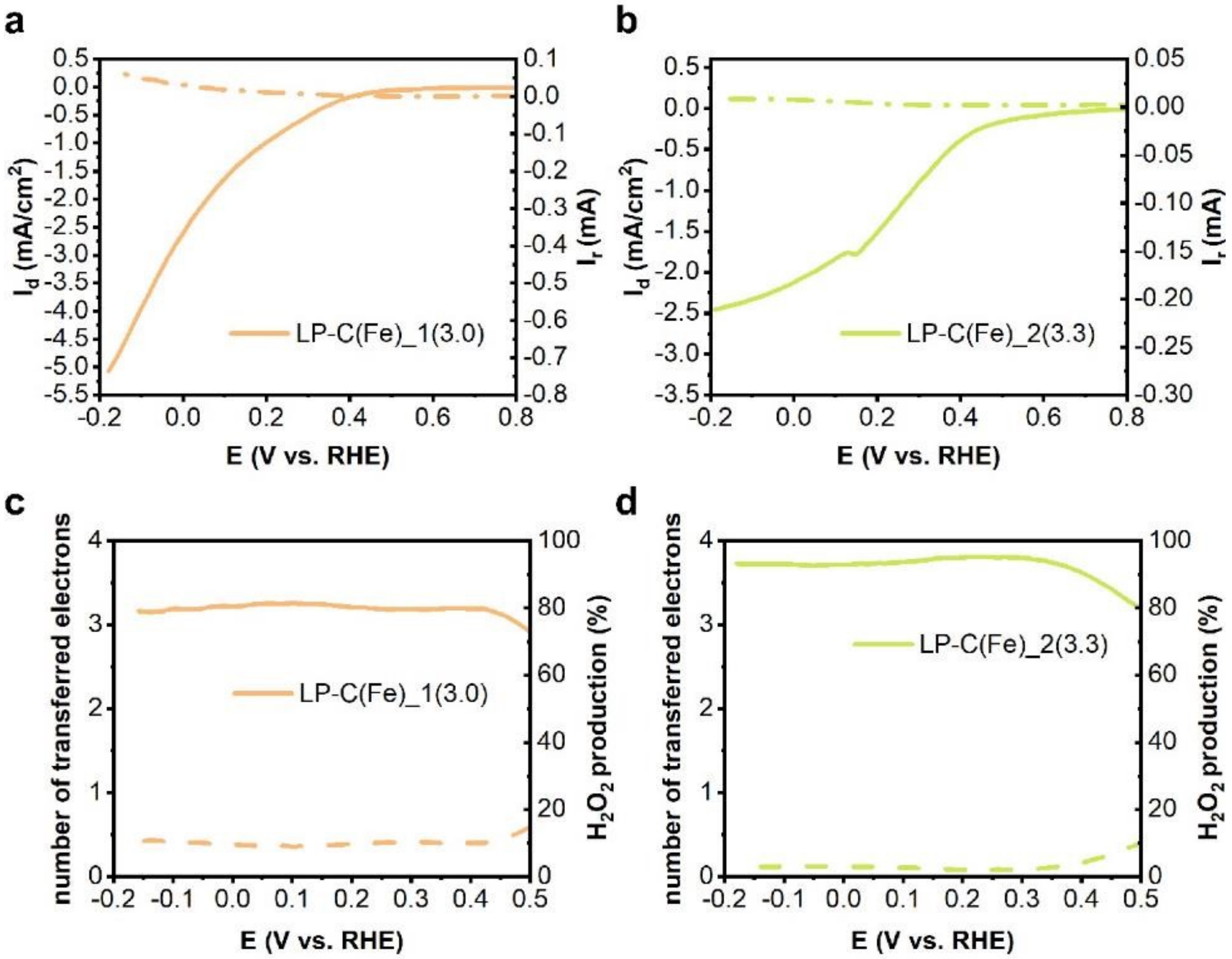

Figure S13. *ORR performance in oxygen saturated 0.5M phosphate buffer (pH 7.2) evaluated using an RRDE setup. (a) and (b) Linear sweep voltammetry of LP-C(Fe)_1(3.0) and LP-C(Fe)_2(3.3), (c) and (d) Calculated number of transferred electrons and H_2O_2 production efficiency of LP-C(Fe)_1(3.0) and LP-C(Fe)_2(3.3). H_2O_2 ring current and selectivity (%) in dashed lines*

Comparison with published studies

Table S4. *Overview of onset potentials and H_2O_2 production efficiencies of previously published and our materials in alkaline electrolyte. The onset potential was calculated by the intercept with X-axes of the tangent to the LSV curve at E1/2. The values in Table S4 are either given in the text or estimated from the data given in each manuscript.*

Sample	Fe type	Onset potential (V vs. RHE)	Mechanism	max. H_2O_2 prod	Ref.
CA/U300	-	0.73	2 e^-	60	this work
LP-C(Fe)_2(3.3)	α-Fe_2O_3/FeO/Fe(0)@LP_C	0.77	2 e^-	80	this work
LP-C(Fe)_2(14.5)	α-Fe_2O_3/FeO/Fe(0)@LP_C	0.72	4 e^-	8	this work
Fe-CNT	Fe-C-O	0.82	2 e^-	95	1
CG400	-	0.72	2 e^-	93	2
O-CNT	-	0.73	2 e^-	93	3
Fe_3O_4-graphene	Fe_3O_4 nanoparticles	0.74	2 e^-	80	4
CeO_2/C	-	0.75	2 e^-	44	5
SnNi/C	-	0.70	2 e^-	88	6
Fe_3O_4@NT	Fe_3O_4		2 e^-		7
NC@Fe_2O_3-CNT	γ-Fe_2O_3, Fe-N_x, and Fe_5C_2	0.96	2 e^-	97.3	8
Fe_2O_3	(001) Fe_2O_{3-x}	0.73	2 e^-	100	9
Fe_2O_3	(012) Fe_2O_{3-x}	0.84	-	10	
α-Fe_2O_3/g-C_3N_4	α-Fe_2O_3		2 e^- and 4 e^-	20	10
Fe_3O_4 NP	Fe_3O_4	-0.6 V vs. SCE (pH 8.5)	2 e^- and 4e^-	50	11
γ-Fe_2O_3/rGO	γ-Fe_2O_3	0.78	2+2 e^-	-	12
LP-C(Fe)_1(3.0)	η-Fe_2O_3/Fe(0)	0.77	2 e^- and 4 e^-	40	this work
LP-C(Fe)_1(12.1)	Fe_3O_4	0.80	4 e^-	2	this work
Fe_2O_3/P-S-GC	Fe_2O_3	0.97	4 e^-	-	13
α-Fe_2O_3@NT	α-Fe_2O_3		4 e^-		7
γ-Fe_2O_3@CNF	γ-Fe_2O_3	0.92	4 e^-	-	14
Fe_{SA}/FeO_{NC}/NSC	Fe-N_4 and Fe_2O_3	0.99	4 e^-	15	15
Fe_2O_3/N-PCs-850	Fe_2O_3	0.936	4 e^-	5	16
Fe_2O_3/FeN_x@CNF	Fe_2O_3 and Fe-N	1.10	4 e^-	3	17
Fe_2O_3@CNF	Fe_2O_3	1.06	4 e^-	20	
Fe-Fe_2O_3@NGr	Fe(0), Fe_2O_3, and Fe-N	0.075 V vs. Hg/HgO		13	18
Fe-Fe_2O_3@RGO	Fe(0) and Fe_2O_3	-0.07 V vs. Hg/HgO		51.2	
Fe_2O_3@Fe-N-C-800	Fe_2O_3 and Fe-N	1.02	4 e^-	-	19
Fe/Fe_2O_3/Fe_3C@N-CNT	Hollow particles Fe/Fe_2O_3/Fe_3C	0.90	4 e^-	2	20
Fe-CNSs-N	α-Fe_2O_3 and Fe_3O_4	0.90	4 e^-	-	21
FeN_x/Fe_2O_3-CNF	γ-Fe_2O_3 and Fe-N	0.87	4 e^-	6	22
Fe_2O_3/N-bio-C	Fe_2O_3	0.90	hybrid	-	23
Fe and N co-doped C	Fe-N-C	0.51 (neutral pH)	4 e^-	-	24
OMCS-Fe_2O_3		0.804	4 e^-	-	25
Fe_2O_3@NC-800	γ-Fe_2O_3	0.97	4 e^-	1.20	26
Fe_3O_4 - GO	Fe_3O_4		4 e^-	-	27
Fe_2O_3/GO	Fe_2O_3	0.85	2+2e^-	-	28
Fe/N-CNTs	Fe-N	0.862	4 e^-		29
P-Fe-C-900	P-Fe-C	0.825	4 e^-	15	30
Hemin/NPC-900	Fe-N-C	0.99	4 e^-	-	31
Fe@N/HCS	Fe_3O_4	0.90	4 e^-	15	32
Fe_3O_4@NHCS	Fe_3O_4	0.9	4 e^-	-	33
Fe_3O_4/Fe_3C@NC-1	Fe_3O_4 and Fe_3C	0.97	4 e^-	10	34
Fe_3O_4 NPs/NGC	Fe_3O_4	1.015	4 e^-	9	35
COP@K10-Fe-900	Fe_3O_4 and Fe-N-C	0.97	4 e^-	10	36
Fe_3O_4@NGA	Fe_3O_4	0.92	4 e^-	-	37
Fe_3O_4/FeNSG-3	Fe-N-C and Fe_3O_4	0.951	4 e^-	6	38
C-FePPDA-900	Fe_3O_4 with o-vacancies on n-doped carbon	0.87	4 e^-	7.5	39
Fe_3O_4@FeNC	Fe_3O_4 and Fe-N		4 e^-	2	40
Fe_3O_4/NCMTs-800(IL)	Fe_3O_4	0.794	4 e^-	-	41

References

1 K. Jiang, S. Back, A. J. Akey, C. Xia, Y. Hu, W. Liang, D. Schaak, E. Stavitski, J. K. Nørskov, S. Siahrostami and H. Wang, *Nat. Commun.*, 2019, **10**, 3997.

2 Y.-H. Lee, F. Li, K.-H. Chang, C.-C. Hu and T. Ohsaka, *Appl. Catal. B Environ.*, 2012, **126**, 208–214.

3 Z. Lu, G. Chen, S. Siahrostami, Z. Chen, K. Liu, J. Xie, L. Liao, T. Wu, Di. Lin, Y. Liu, T. F. Jaramillo, J. K. Nørskov and Y. Cui, *Nat. Catal.*, 2018, **1**, 156–162.

4 W. R. P. Barros, Q. Wei, G. Zhang, S. Sun, M. R. V Lanza and A. C. Tavares, *Electrochim. Acta*, 2015, **162**, 263–270.

5 M. H. M. T. Assumpção, A. Moraes, R. F. B. De Souza, I. Gaubeur, R. T. S. Oliveira, V. S. Antonin, G. R. P. Malpass, R. S. Rocha, M. L. Calegaro, M. R. V Lanza and M. C. Santos, *Appl. Catal. A Gen.*, 2012, **411**–**412**, 1–6.

6 V. S. Antonin, M. H. M. T. Assumpção, J. C. M. Silva, L. S. Parreira, M. R. V Lanza and M. C. Santos, *Electrochim. Acta*, 2013, **109**, 245–251.

7 Y. Xue, W. Jin, H. Du, S. Wang, S. Zheng and Y. Zhang, *RSC Adv.*, 2016, **6**, 41878–41884.

8 X. Cheng, S. Dou, G. Qin, B. Wang, P. Yan, T. T. Isimjan and X. Yang, *Int. J. Hydrogen Energy*, 2020, **45**, 6128–6137.

9 R. Gao, L. Pan, Z. Li, C. Shi, Y. Yao, X. Zhang and J.-J. Zou, *Adv. Funct. Mater.*, 2020, **30**, 1910539.

10 S. Dutta, T. K. Jana, R. Maiti, K. De and K. Chatterjee, *ChemistrySelect*, 2021, **6**, 11759–11767.

11 Y. Xiao, J. Hong, X. Wang, T. Chen, T. Hyeon and W. Xu, *J. Am. Chem. Soc.*, 2020, **142**, 13201–13209.

12 Q. Feng, Z. Chen, K. Zhou, M. Sun, X. Ji, H. Zheng and Y. Zhang, *ChemistrySelect*, 2021, **6**, 8177–8181.

13 H. Zhao, J. Wang, C. Chen, D. Chen, Y. Gao, M. Saccoccio and F. Ciucci, *RSC Adv.*, 2016, **6**, 64258–64265.

14 Z. Yao, Y. Li, D. Chen, Y. Zhang, X. Bao, J. Wang and Q. Zhong, *Chem. Eng. J.*, 2021, **415**, 129033.

15 Y. Lei, F. Yang, H. Xie, Y. Lei, X. Liu, Y. Si and H. Wang, *J. Mater. Chem. A*, 2020, **8**, 20629–20636.

16 T. Zhang, L. Guan, C. Li, J. Zhao, M. Wang, L. Peng, J. Wang and Y. Lin, *Catalysts*, 2018, **8**, 101.

17 M. Wang, T. Liao, X. Zhang, J. Cao, S. Xu, H. Tang and Y. Wang, *Adv. Mater. Interfaces*, 2022, **9**, 2101904.

18 V. M. Dhavale, S. K. Singh, A. Nadeema, S. S. Gaikwad and S. Kurungot, *Nanoscale*, 2015, **7**, 20117–20125.

19 X. Xu, C. Shi, Q. Li, R. Chen and T. Chen, *RSC Adv.*, 2017, **7**, 14382–14388.

20 B. Zhang, T. Li, L. Huang, Y. Ren, D. Sun, H. Pang, J. Yang, L. Xu and Y. Tang, *Nanoscale*, 2021, **13**, 5400–5409.

21 Y. Wang, R. Gan, H. Liu, M. Dirican, C. Wei, C. Ma, J. Shi and X. Zhang, *J. Mater. Chem. A*, 2021, **9**, 2764–2774.

22 Q. Yu, S. Lian, J. Li, R. Yu, S. Xi, J. Wu, D. Zhao, L. Mai and L. Zhou, *J. Mater. Chem. A*, 2020, **8**, 6076–6082.

23 Y. Wu, H. Jiao, M. Hou and P. Zhang, *J. Phys. Conf. Ser.*, 2021, **2079**, 12002.

24 Y. Su, H. Jiang, Y. Zhu, W. Zou, X. Yang, J. Chen and C. Li, *J. Power Sources*, 2014, **265**, 246–253.

25 J. He, B. Li, J. Mao, Y. Liang, X. Yang, Z. Cui, S. Zhu and Z. Li, *J. Mater. Sci.*, 2017, **52**, 10938–10947.

26 Z. Xiao, G. Shen, F. Hou, R. Zhang, Y. Li, G. Yuan, L. Pan, J. J. Zou, L. Wang, X. Zhang and G. Li, *Catal. Sci. Technol.*, 2019, **9**, 4581–4587.

27 K. Lellala, *Energy & Fuels*, 2021, **35**, 8263–8274.

28 S. Arya Gopal, A. Edathiparambil Poulose, C. Sudakar and A. Muthukrishnan, *ACS Appl. Mater. Interfaces*, 2021, **13**, 44195–44206.

29 W. Liu, K. Yuan, Q. Ru, S. Zuo, L. Wang, S. Yang, J. Han and C. Yao, *Arab. J. Chem.*, 2020, **13**, 4954–4965.

30 Z. Yang, J. Wu, X. Zheng, Z. Wang and R. Yang, *J. Power Sources*, 2015, **277**, 161–168.

31 Z. Lu, J. Chen, W. Wang, W. Li, M. Sun, Y. Wang, X. Wang, J. Ye and H. Rao, *Small*, 2021, **17**, 2007326.

32 B. Wang, Y. Ye, L. Xu, Y. Quan, W. Wei, W. Zhu, H. Li and J. Xia, *Adv. Funct. Mater.*, 2020, **30**, 2005834.

33 Y. Li, H. Huang, S. Chen, X. Yu, C. Wang and T. Ma, *Nano Res.*, 2019, **12**, 2774–2780.

34 M. Liu, X. Guo, L. Hu, H. Yuan, G. Wang, B. Dai, L. Zhang and F. Yu, *ChemNanoMat*, 2019, **5**, 187–193.

35 Y. Chen, L. Li, X. Liu, W. Wan and J. Luo, *Mater. Res. Express*, 2019, **6**, 65019.

36 J. Guo, Y. Cheng and Z. Xiang, *ACS Sustain. Chem. Eng.*, 2017, **5**, 7871–7877.

37 Z. Liang, W. Xia, C. Qu, B. Qiu, H. Tabassum, S. Gao and R. Zou, *ChemElectroChem*, 2017, **4**, 2442–2447.

38 Y. Li, Y. Zhou, C. Zhu, Y. H. Hu, S. Gao, Q. Liu, X. Cheng, L. Zhang, J. Yang and Y. Lin, *Catal. Sci. Technol.*, 2018, **8**, 5325–5333.

39 Y. Deng, X. Tian, G. Shen, Y. Gao, C. Lin, L. Ling, F. Cheng, S. Liao and S. Zhang, *J. Colloid Interface Sci.*, 2020, **567**, 410–418.

40 S. Hu, W. Ni, D. Yang, C. Ma, J. Zhang, J. Duan, Y. Gao and S. Zhang, *Carbon N. Y.*, 2020, **162**, 245–255.

41 G. Liu, B. Wang, P. Ding, Y. Ye, W. Wei, W. Zhu, L. Xu, J. Xia and H. Li, *J. Alloys Compd.*, 2019, **797**, 849–858.